False Diamond Turning Artifacts in Phase Retrieval Results

Thomas P. Zielinski, James R. Fienup
The Institute of Optics, University of Rochester,
275 Hutchison Rd., Rochester, NY USA 14627

ABSTRACT

Many modern optical designs employ diamond-turned optical components and utilize phase retrieval for metrology during testing, assembly, and commissioning. The accuracy of the wavefronts obtained by phase retrieval depends on the fidelity of the system model used during the retrieval, including knowledge of the pupil amplitude, and the relationship between the digital sample spacing in the pupil and each point spread function (PSF), i.e., the plate scale. However, recent simulations have shown that errors in the estimation of both the plate scale and unknown pupil vignetting can both lead to mid-spatial-frequency groove-like errors in the wavefront maps obtained by phase retrieval. In particular, these errors manifest themselves as concentric rings resembling diamond-turning tooling marks, and can therefore easily confound metrology results involving diamond-turned components. Furthermore it was found that only moderate amounts of pupil vignetting, and errors in sampling ratio as low as 2% produced groove errors consistent in magnitude with typical diamond-turning specifications. This paper presents the results of this study on the magnitude and nature of these artifacts and their impact on telescope metrology.

Keywords: Phase retrieval, diamond turning, metrology, wavefront sensing

1. INTRODUCTION

Single-point diamond turning is a computed numerically controlled (CNC) machining process often used in the manufacture of precisions optical components. It is particularly useful for generating high quality aspherical surfaces, and is often utilized to machine the crystalline materials used in IR optics. As a result, diamond-turned components are often found in astronomical systems and their associated science instruments. Simultaneously, phase retrieval has becoming an increasingly important metrology technique used during the testing and commissioning of such systems. For example, focus-diverse phase retrieval is one of the primary metrology tools used during the integration and commissioning of the James Webb Space Telescope (JWST),[1] which contains instruments with several different IR crystalline materials,[2] and diamond-turned optical components.[3] Therefore it is important to understand the capability of phase retrieval to sense the mid-spatial frequency wavefront errors typically left by diamond turning processes. This paper will present recent simulation results showing how false mid-spatial frequency phase errors resembling diamond tooling marks can appear in phase retrieval results in the presence of a model mismatch.

2. PHASE RETRIEVAL BACKGROUND

Focus-diverse phase retrieval has become an increasingly powerful metrology tool in recent years,[4] and is often used in situations where conventional metrology techniques are impractical or prohibitively complicated. Phase retrieval replaces the hardware complexity associated with conventional metrology with software algorithms, which has several key advantages in addition to experimental simplicity. Phase retrieval removes the need for precision manufactured and calibrated reference optics. Additionally, phase retrieval has the ability to measure the system at various stages of manufacturing and assembly, in environments inhospitable to conventional metrology, and often utilizes the system's existing in-situ detector array.

The input to focus-diverse phase retrieval algorithms are point spread functions (PSFs) with a known defocus, along with a few key first-order parameters such as the illumination profile in the pupil, effective focal length, wavelength, and detector pixel spacing. The software uses this information to generate a model of the electric field, including the

estimated phase, in the pupil and numerically propagate it to the planes where PSF data was collected. Depending on the particular approach, an iterative transform algorithm,[5] or a nonlinear optimization algorithm[6] is then used to modify the phase until the numerically computed PSFs agree with the measured PSFs. The same algorithms can be used to optimize over the amplitude of the field in the pupil plane as well.

In practice, a Fresnel diffraction model,[7] implemented with a discrete Fourier transform (FFT), is often used to perform the propagation of the electric field from the pupil to the PSF domain. The numerical implementation of this propagator imposes a fixed sampling relationship between these two domains,

$$Nd_{\xi} = \frac{\lambda f}{d_x} , \qquad (1)$$

where λ is the wavelength, f is the focal length, N is the number of FFT samples, and d_{ξ}, d_x are the sample spacings in the pupil and image planes, respectively. The sampling of a pupil of diameter D can be written in terms of a single dimensionless parameter, the sampling ratio, Q, which expresses the degree of under-sampling or over-sampling relative to the Nyquist rate of the optical field,

$$Nd_{\xi} = QD. \qquad (2)$$

In this notation, $Q < 1$ represents an undersampled system, $Q = 1$ corresponds to a system that is Nyquist sampled for the complex amplitude of the optical field, and $Q = 2$ is a system that is Nyquist sampled for intensity. Combining Equations (1) and (2) yields

$$Q = \frac{\lambda F/\#}{d_x}, \qquad (3)$$

where $F/\# = f/D$. In this framework, Q is a single number which determines the scaling of the propagation in the Fourier kernel of the Fresnel transform.

Several different methods for determining the Q of a system exist. First-order design parameters can be used with Equation 3 to calculate Q; however there are typically uncertainties in the knowledge of these values in the as-built system. If there is confidence in the knowledge of the focal length and wavelength, a pupil imaging lens can be used to determine the size of the pupil and equivalently Q. In situations with simple pupils and high signal-to-noise ratio (SNR), Q can be determined directly from the cutoff of the modulation transfer function.[8,9] Additional hardware, such as non-redundant masks in the pupil can also be used to directly measure plate scale.

Unlike the other parameters such as pupil phase, pupil amplitude, and the focus diversity that are typically retrieved during the course of a phase retrieval algorithm, there is currently no simple way to directly optimize for Q. Furthermore, it has been observed that errors in the estimation of the sampling ratio lead to mid-spatial-frequency groove-like errors in the wavefront maps obtained by phase retrieval. In particular, these errors manifest themselves as concentric rings resembling diamond-turning tooling marks, and can therefore easily confound metrology results involving diamond-turned components.

3. SIMULATION

A simulation was run to determine the effect of a mismatch in Q on the fidelity of the retrieval. A smooth random phase map was generated with parameters outlined in Table 1. The simulated phase and simulated amplitude are shown in Figure 1.

Table 1. Simulation Parameters

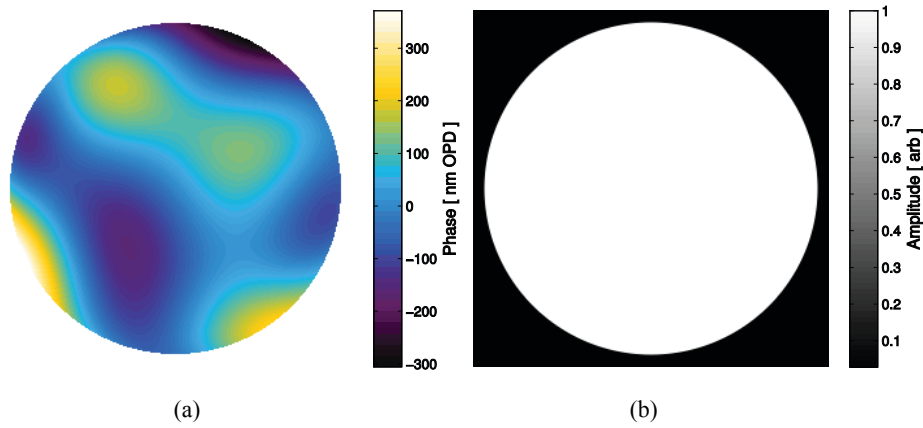| Parameter	Value(s)
Simulation Wavelength	2μm
Number of Zernike Polynomials	36
Pupil Aberrations	100nm OPD RMS
Simulated Q	2
Number of PSFs	4
Focus Diversity	-8, -4, 4, 8 waves P-V

(a)   (b)

Figure 1. (a) Simulated phase, (b) simulated amplitude.

Point-spread functions corresponding to this phase and amplitude were generated with a noise model corresponding to a commercially available CCD detector operating at 80% of full well. The detector noise parameters used are summarized in Table 2. The phase and amplitude were then retrieved from these point-spread functions using a nonlinear optimization-based phase retrieval algorithm[6] with an error metric insensitive to bias and gain.[10] Piston, tip, tilt, and focus terms were removed from all wavefront maps in this paper to aide in comparison.

Table 2. Detector Noise Characteristics

Description of Stochastic Error	Value(s)	Units
Read Noise	16	electrons rms
Dark Current	0.5	electrons
Photon Noise	32×10^3	photons in peak pixel
Detector Quantization	12	bits

4. RESULTS

4.1 Mismatch in Q

The phase retrieval algorithm was run on the simulated data with an intentional mismatch in the modeled Q value, and the RMS value of the residual phase (simulated phase – retrieved phase) was computed. Figure 2 shows the results of this simulation.
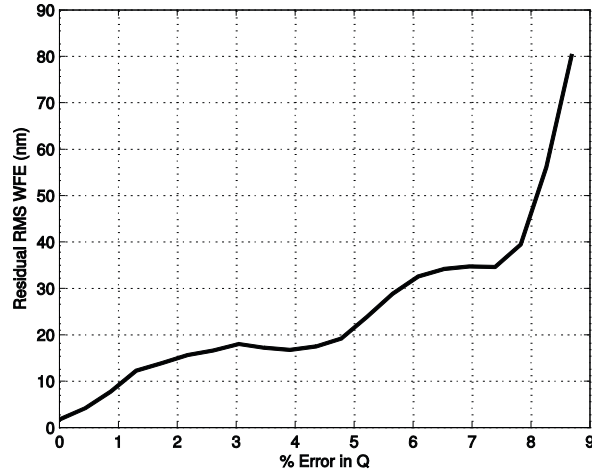

Figure 2. RMS of the residual phase as a function of error in Q.

As expected, the magnitude of the retrieved wavefront errors increase as errors in the estimated value of Q become worse. The graph shows that even minor errors in the estimate of Q introduce wavefront errors comparable in magnitude to diamond turning specifications.

Of particular interest is the nature of the errors in the retrieved phase. The residual phase error and recovered amplitude corresponding to a 5% error in Q are shown in Figure 3. Visual examination of this residual reveals a quasi-centro-symmetric ring-like artifact in both the phase and amplitude which can interfere with the ability to measure the surface quality of a diamond-turned part or be misinterpreted as a diamond-turning error where there is none.

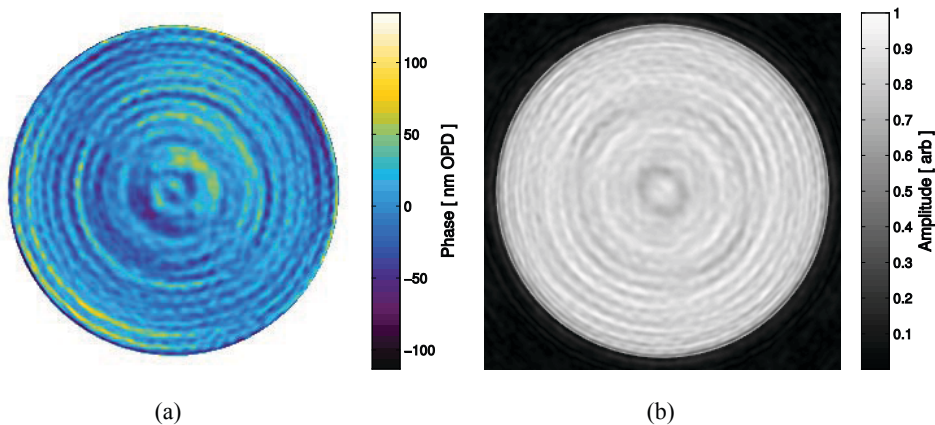(a)   (b)

Figure 3. (a) Residual phase after retrieval, (b) retrieved pupil amplitude.

4.2 Unknown Vignetting

The simulation was re-run with perfect knowledge of Q, but on PSFs generated from a pupil vignetting unknown to the algorithm. Physically, the effect of a vignetted pupil is qualitatively similar to shrinking the diameter of the pupil, thereby changing Q. However, since the algorithm is able to retrieve amplitude, it should be able to compensate for this error. The amplitude used to simulate the PSFs had an approximately 50% rolloff at the edge of the pupil, and is shown in Figure 4. The phase retrieval algorithm was started with a flat illumination pattern.
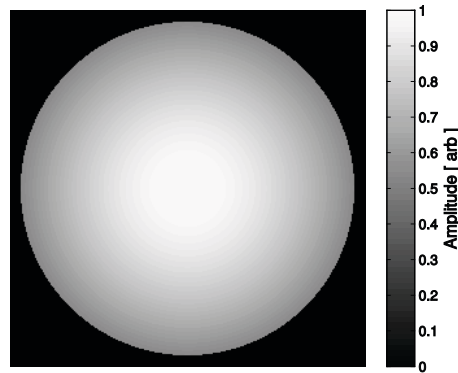

Figure 4. Simulated pupil amplitude.

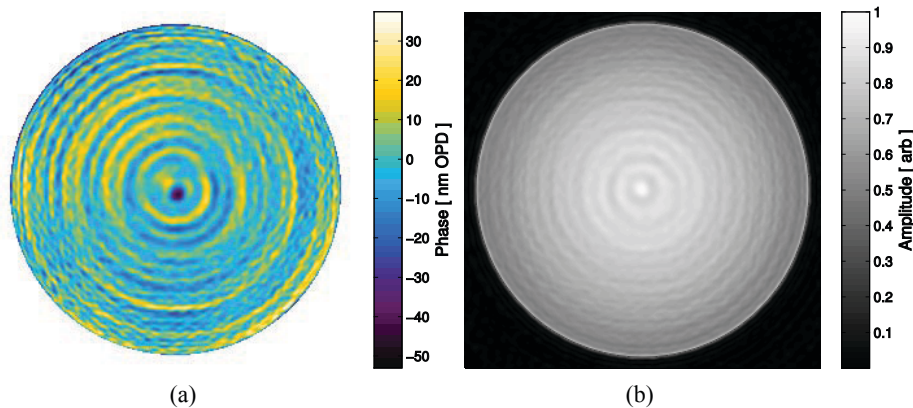The results of the retrieval are shown in Figure 5.

Figure 5. (a) Residual phase after retrieval, (b) retrieved pupil amplitude.

While the algorithm was able to approximately retrieve the vignetting in the pupil, mid-spatial frequency groove errors with an RMS of 9 nm OPD were still introduced in the residual phase. This is likely due to the fact that phase and amplitude are both being optimized simultaneously, allowing the algorithm to arrive at a local minima which does not reflect the true amplitude and phase of the system.

5. CONCLUSION

Model mismatches corresponding to both unknown vignetting and sampling ratio errors introduce quasi-centro-symmetric, ring-like, mid-spatial frequency errors in the retrieved phase that resemble diamond turning artifacts. In fact, errors in the sampling ratio as low as 2% produced groove errors consistent in magnitude with diamond-turning specifications. Therefore, additional care needs to be taken in accurately measuring the pupil illumination pattern and Q of a system when trying to characterize mid-spatial frequency errors using phase retrieval. This is particularly true of systems having unpolished diamond-turned components where phase retrieval is used to validate surface quality requirements.

REFERENCES

[1] J. Nella, P. D. Atcheson, C. B. Atkinson, D. Au, A. J. Bronowicki, E. Bujanda, A. Cohen, D. Davies, P. A. Lightsey, and R. Lynch, "James Webb Space Telescope (JWST) Observatory Architecture and Performance," Proc. SPIE **5487**, 576 (2004).

[2] E. Kvamme, J. Earthman, D. Leviton, and B. Frey, "Lithium Fluoride Material Properties as Applied on the NIRCam Instrument," Proc. SPIE **5904**, 212-221 (2005).

[3] P. Shore, P. Morantz, D. Lee, and P. McKeown, "Manufacturing and Measurement of the MIRI Spectrometer Optics for the James Webb Space Telescope," CIRP Annals-Manufacturing Technology **55,** 543-546 (2006).

[4] G. R. Brady, and J. R. Fienup, "Measurement Range of Phase Retrieval in Optical Surface and Wavefront Metrology," Appl. Opt. **48,** 442-449 (2009).

[5] J. R. Fienup, "Phase Retrieval Algorithms: a Comparison," Appl. Opt. **21,** 2758-2769 (1982).

[6] J. R. Fienup, "Phase Retrieval Algorithms for a Complicated Optical System," Appl. Opt. **32,** 1737-1746 (1993).

[7] J. W. Goodman, *Introduction to Fourier Optics* 3rd Ed. (Roberts & Company Publishers, 2005).

[8] B. H. Dean, "Determining Phase Retrieval Sampling from the Modulation Transfer Function," NASA GSFC Technology Disclosure, GSC-15934-1, Sept. 1, 2009.

[9] B. H. Dean, "Phase Retrieval Results using NIRCam Updated Diamond Turning Data," NASA GSFC Technical Memorandum, Jan. 24, 2009.

[10] S. T. Thurman, and J. R. Fienup, "Phase retrieval with Signal Bias," J. Opt. Soc. Am. A **26,** 1008-1014 (2009).